Published in final edited form as:
Clin Exp Metastasis. 2009 ; 26(7): 729–738. doi:10.1007/s10585-009-9272-9.

Evaluation of pulsed high intensity focused ultrasound exposures on metastasis in a murine model

Hilary Hancock and **Matthew R. Dreher**
Department of Radiology and Imaging Sciences, Clinical Center, National Institutes of Health, Bethesda, MD 20892, USA

Nigel Crawford and **Claire B. Pollock**
Laboratory of Cancer Biology and Genetics, Center for Cancer Research, National Cancer Institute, Bethesda, MD 20892, USA

Jennifer Shih and **Bradford J. Wood**
Department of Radiology and Imaging Sciences, Clinical Center, National Institutes of Health, Bethesda, MD 20892, USA

Kent Hunter
Laboratory of Cancer Biology and Genetics, Center for Cancer Research, National Cancer Institute, Bethesda, MD 20892, USA

Victor Frenkel
Department of Radiology and Imaging Sciences, Clinical Center, National Institutes of Health, Bethesda, MD 20892, USA

Molecular Imaging Lab, Radiology and Imaging Sciences, Clinical Center, National Institutes of Health, Building 10, Room 1N306a, 10 Center Drive, Bethesda, MD 20892, USA

Abstract

High intensity focused ultrasound (HIFU) may be employed in two ways: continuous exposures for thermal ablation of tissue (>60°C), and pulsed-exposures for non-ablative effects, including low temperature hyperthermia (37–45°C), and non thermal effects (e.g. acoustic cavitation and radiation forces). Pulsed-HIFU effects may enhance the tissue's permeability for improved delivery of drugs and genes, for example, by opening up gaps between cells in the vasculature and parenchyma. Inducing these effects may improve local targeting of therapeutic agents, however; concerns exist that pulsed exposures could theoretically also facilitate dissemination of tumor cells and exacerbate metastases. In the present study, the influence of pulsed-HIFU exposures on increasing metastatic burden was evaluated in a murine model with metastatic breast cancer. A preliminary study was carried out to validate the model and determine optimal timing for treatment and growth of lung metastases. Next, the effect of pulsed-HIFU on the metastatic burden was evaluated using quantitative image processing of whole-lung histological sections. Compared to untreated controls (2/15), a greater number of mice treated with pulsed-HIFU were found to have lungs “overgrown” with metastases (7/15), where individual metastases grew together such

vfrenkel@cc.nih.gov.

that they could not accurately be counted. Furthermore, area fraction of lung metastases (area of metastases/area of lungs) was ~30% greater in mice treated with pulsed-HIFU; however, these differences were not statistically significant. The present study details the development of an animal model for investigating the influence of interventional techniques or exposures (such as pulsed HIFU) on metastatic burden.

Keywords

Pulsed-high intensity focused ultrasound; Mvt-1; Metastasis; Image processing; Metastatic burden

Introduction

Similar to light waves, ultrasound waves may be focused onto relatively small volumes, greatly increasing their intensity. These high intensity focused ultrasound (HIFU) beams allow energy to be deposited deep inside the body, where the waves pass through the skin and intervening tissues, over a wide area, causing fewer or no demonstrable effects. HIFU exposures can be targeted to specific organs, tissues, and tumors with image guidance from diagnostic ultrasound and magnetic resonance imaging (MRI) [1].

HIFU exposures have been generally categorized according to two effects, direct ablation and enhanced (adjuvant) delivery of therapeutics (drugs or gene vectors) [2]. Ablation is the most widespread application of HIFU, utilizing relatively long, continuous exposures in order to generate substantial temperature elevations (e.g. increases of 30–40°C) to cause thermal (i.e. coagulative) necrosis in the tissue. Exposures such as these induce coagulative necrosis resulting in permanent cell death, and are presently being used to treat uterine fibroids and prostate cancer world-wide [1]. Clinical trials are underway to treat breast and kidney tumors [3], as well as liver [4] and testicular cancer [5]. These types of exposures are also being evaluated for reducing pain and alleviating symptoms in patients with bone cancer [6]. Compared to more invasive surgical and interventional procedures, there are many potential advantages to using extra-corporeal HIFU exposures, including limited blood loss and infection, less scar formation, less risk and recovery inherent to surgery and anesthesia, and the non-invasive nature lends itself to out-patient therapy [1].

In comparison to continuous HIFU exposures used for thermal ablation, pulsed exposures can reduce the temporal average intensity and buildup of heat through non-continuous energy deposition [7]. These exposures produce effects through non-thermal mechanisms (e.g. acoustic cavitation and radiation forces) such as structural alterations that can alter tissue permeability. Occurring at both the cellular and macroscopic level, these effects can improve local and systemic delivery, and consequently, the efficacy of various therapeutic agents [2]. Prior reports with murine tumor models showed improved delivery of monoclonal antibodies [8] and enhanced growth inhibition using the proteasome inhibitor bortezomib [9], and plasmid DNA encoding for tumor necrosis factor alpha (TNFα) [10]. Shock wave lithotripsy also employs pulses of focused ultrasound, where relatively higher amplitudes are used over shorter pulse durations. Whereas these exposures have traditionally

been used to treat calculi in the kidneys and the urinary tract [11], they have also been investigated for enhancing gene delivery into tumors [7].

Despite the potential benefit of pulsed-HIFU exposures as an adjuvant cancer therapy, concerns have been raised about potential deleterious effects. Mechanistic studies, for example, in muscle using pulsed HIFU have shown that the exposures can cause reversible structural effects such as increased gaps and disruption of connective tissue between muscle fiber bundles, where these effects are directly correlated with improved convective interstitial transport [12]. Similar effects may be occurring in tumors between parenchymal cells and the extra-cellular matrix, potentially enabling improved transport of therapeutic agents [2]. One potentially undesirable outcome of such an effect would be facilitating the movement of cells in the primary tumor or chemotactic factors and potentially increasing the dissemination of these cells and metastatic burden.

To date, a small number of preclinical and clinical studies have only partly addressed this issue. In one clinical study, tumor lesions in the liver were completely ablated using continuous HIFU exposures. Reverse transcriptase polymerase chain reaction (RT-PCR) was used to detect circulating tumor cells in the patient before and after exposures. It was concluded that complete HIFU ablation did not enhance the potential risk of metastases in patients with solid malignancies [13]. These results were not surprising given that the thermal ablation process essentially `fixes' the tissue in situ, with potentially some mechanical effects occurring on the margin of the focal zone of the HIFU beam [1]. In a preclinical study, similar results were found for ablative exposures in a highly metastatic prostate cancer line, implanted into the hind leg of rats, where increases in the number of lung metastases were not observed [14]. Furthermore, lower diagnostic levels of ultrasound exposures were not found to enhance metastases [15, 16]. In contrast, a study using non-thermal, high-amplitude ultrasound exposures (on subcutaneous tumors implanted into the hind leg of mice) did show a significant increase in the number of lung metastases, when compared to diagnostic ultrasound exposures. These results could be attributed to mechanical effects (i.e. acoustic cavitation), which perhaps were sufficient to physically enhance dissemination of cells from the primary tumor [15]. The high impact of shock waves similarly showed increased metastatic burden in treated mice compared to untreated controls [17, 18]. Overall, studies aimed directly at investigating the effects of HIFU on metastases have been limited, especially pertaining to pulsed-HIFU. In light of this, we proposed to study the consequences of our specific pulsed-HIFU exposures on solid malignancies in mice to determine if they could be affecting metastasis.

In order to evaluate the effect of HIFU exposures, the highly metastatic murine mammary tumor cell line, Mvt-1, was chosen. This has previously been used for quantitative studies due to its characteristically high visibility of lung metastases [19, 20]. This model was also chosen because of the ability to grow the primary tumor subcutaneously in the hind flanks of mice, which facilitates treatment with pulsed-HIFU in a safe and efficient manner [8, 9, 21]. A preliminary study was first carried out to determine the optimum period for primary tumor growth before treatment, as well for subsequent development of the lung metastases. A quantitative technique was then developed using image processing of histological sections in order to evaluate the influence of pulsed-HIFU on metastatic burden.

Materials and methods

Animal model

All animal work was performed in compliance with institutional animal care and use committee (IACUC) guidelines, and according to an animal study protocol approved by the NIH Clinical Center ACUC. Adult (6–8 weeks old) female FVB/NJ mice were purchased from The Jackson Laboratory (Bar Harbor, Maine). Animals were housed 5 per cage, exposed to 12 h cycles of light and darkness, and given free access to standard food pellets and water. They were given a minimum of 2 days of acclimation time after arriving at our facilities prior to the start of the study.

Cell line

The Mvt-1 cell line, which is derived from an explant-cell culture of primary mammary tumors from MMTV-c-Myc/MMTV-Vegf bi-transgenic mice [19], was generously provided by Dr Michael Johnson of the Lombardi Cancer Center at Georgetown University. The cells were cultured in Dulbecco's Modification of Eagle's Medium (DMEM; Cellgro, Herndon, VA) containing 10% fetal bovine serum (FBS; Cellgro, Herndon, VA), with culture medium being replaced at 2–3 days intervals. When the cells achieved near confluency, they were washed once with 5 ml phosphate-buffered saline solution (PBS), incubated with 2 ml trypsin-EDTA for 5 min, and passaged at a 1:30 dilution into a fresh culture flask [19].

Subcutaneous tumor inoculation

Cultured Mvt-1 cells were dissociated from culture plates with trypsin, washed and resuspended in PBS. About 10^5 cells per 100 μl were injected subcutaneously in the right thigh of mice [22]. This resulted in tumors whose growth could be easily monitored and which were accessible to HIFU treatments. Tumors were measured three times a week with a digital caliper; tumor volume was calculated as $V = (\text{length} \times \text{width}^2)/2$.

HIFU system

A custom built, image guided, HIFU system, modified from a Sonoblate® 500 (Focus Surgery, Indianapolis, IN), was used to provide all exposures. The probe possessed a spherical, concave 1 MHz therapeutic transducer (5 cm diameter; focal length 4 cm) and a collinear, 10 MHz imaging transducer (8 mm aperture). The focal zone of the therapeutic transducer was in the shape of an elongated ellipsoid, with an axial length (−3 dB) of 7.2 mm and radial diameter (−3 dB) of 1.38 mm.

Pulsed-HIFU exposures

Pulsed-HIFU exposures were carried out as previously described [8, 9, 21]. In short, mice were anesthetized with inhalation isofluorane (2%; O_2 1 l/h) and respiration was monitored throughout the procedure. Prior to exposure, skin on and around tumor was shaved and depilated. The mouse was placed in a plastic holder, with its head in an anesthesia cone, and secured using Transpore™ surgical tape (3M™, St. Paul, MN). The tumor was positioned to face outward, away from the holder. The holder was then mounted onto a 3D movable stage and the mouse, positioned vertically, was placed into a degassed water bath maintained at

36°C, with its head above the water level. Using the stage while scanning with the imaging transducer, the mouse was positioned so that the tumor was directly within the focal zone of the transducer. The axial center of the focal zone was positioned at the center of the tumor's depth (*z* dimension), such that the energy of the exposures was concentrated in the tumor and the diverging beam passed through the underlying muscle. Treating the tumors in this manner was not previously found to have any detrimental effects on the muscle tissue [8]. The rastering sequence of treatment in the *x* and *y* plane was designated in a grid pattern, with a lateral (*x*) and vertical (*y*) spacing of 2 mm between raster points. The following parameters were used for all exposures in the study: total acoustic power: 40 W (spatial averaged intensity = 2,685 W cm^{-2}; peak rarefractional pressure = 8.95 MPa); pulse repetition frequency: 1 Hz; duty cycle: 5% (50 ms ON; 950 ms OFF); 100 pulses at each raster point. The cumulative HIFU exposure lasted, on average, 15 min depending on the tumor size. The mice in the control group were prepared similarly to those receiving pulsed-HIFU, but instead were given sham exposures (0 W). Mice from both control and treated groups were removed from the water bath, dried, and placed in a warmed recovery cage and monitored before being returned to their group cages in the animal holding facility.

Survival surgery

At 24 h post HIFU, the primary tumor of both treated and control groups was surgically removed as previously described [23]. In brief, the tumor bearing limb was removed by disarticulation at the hip joint. The femoral artery and vein were tied off with 3−0 coated Vicryl™ suture (Ethicon, Somerville, NJ) prior to separation. If needed, additional hemostasis was performed with Vet-Bond™ tissue adhesive (3 M, St. Paul, MN). Surgical wounds were closed using 9 mm surgical wound clips (Clay Adams®, Sparks, MD) and, if needed, sutures were used. Saline (0.5 ml) was administered subcutaneously to mice prior to surgery. Intraperitoneal buprenorphine analgesia SQ (0.2 ml) was administered prior to, and 4 h post surgery. After surgery, animals were moved to pre-warmed recovery cages and monitored before being placed into clean cages. Skin closures were removed 10 days post surgery.

Experimental studies

Characterization of metastases—In order to evaluate and characterize metastatic growth of the Mvt-1 murine breast cancer model in vivo, a preliminary study was performed. Mice were inoculated for primary tumor growth, underwent surgery at 1, 2 and 3 weeks post inoculation (primary tumor growth period), and euthanized at varying time points after surgery (metastases growth period) (Fig. 1a). Histological sections were made of the lungs and the number of metastases in each lung was counted at 100× magnification using light microscopy (Olympus, Center Valley, PA). The lungs were further characterized based on the histology with regards to the percentage of mice that did not have metastases or had lungs that were too overgrown with metastatic growth so that an accurate count of metastases could not obtained. Overgrowth was defined as relatively large and non-uniform lesions (compared to typical isolated lesions) that appeared to be made up of individual lesions that had grown into one another. Pairs of mice were used for each combination of primary tumor and metastases grow out periods.

Evaluation of HIFU on metastases—The results from the preliminary study indicated that the most consistent metastatic burden was observed when surgeries were performed at 2 weeks post inoculation, and then the metastases were allowed to grow out for another 2 weeks. Based on these results, mice were given pulsed-HIFU exposures (real & sham) at 2 weeks post inoculation, and underwent surgery 24 h later. 15 mice were used for each group. The mice were euthanized 2 weeks post treatment (Fig. 1b). Digital images of histological sections of the lungs were captured and images analyzed.

Histology

Harvested lung samples were fixed in 10% formalin, dehydrated in graded ethanol, embedded in paraffin, sectioned, placed on glass slides, deparaffinized in xylene, rehydrated in graded ethanol, and stained with hematoxylin and eosin [22]. Three parallel sections were made, uniformly through the lungs.

Digital capture of histological sections

H&E stained tissues were imaged with bright field microscopy using a microscope equipped with an AxioCam MRc 5 color CCD camera, motorized stage, and automated image acquisition software (Zeiss, Axio Imager. M1, Thornwood, NY). The images were acquired in a tile fashion and later stitched together into a mosaic using software provided by the manufacturer (final image resolution = 0.68 μm). These images were exported and archived as 8-bit RGB TIFFs.

Image analysis

Custom image processing code was written in Matlab (MathWorks, Natick, MA) to isolate the metastases area fraction and size of each individual lesion. The lung tissue was isolated by thresholding the red channel. The non-selected holes within the lung tissue were filled in to represent the total area of the lung tissue. The area occupied by metastatic lesions was extracted from the blue channel by assuming that the nuclei density was greater within a lesion than in normal lung tissue. A circle with a diameter of 75 μm was passed over the image and its contents were analyzed. The location at the circle's center was designated a metastatic lesion if the sum of its area occupied by nuclei was greater than 65%. The holes within the met positive area of the metastatic lesion were similarly filled as the lung tissue. Metastases area fraction was calculated by dividing the metastases area by the lung area. The size and number of each individual lesion was archived in a spread sheet for later analysis. Note, since a clinically relevant metastasis size is unknown, metastases were included in the overall metastatic burden above four cutoff limits; 0.001, 0.10, 0.25, and 0.50 mm^2.

Statistical analysis

A paired student's *T*-test was carried out to determine if a difference in the evaluated indicators of metastatic burden were significant between control and treated mice. A *P*-value of <0.05 was considered significant.

Results

Primary tumor growth

At the time of resection, primary tumors ranged in volume from 59.9 to 268.4 mm^3 with an average volume of 139.8 mm^3 and a standard deviation of 53.99 mm^3. Tumor volume at the time of resection had no significant influence on the metastatic burden in the lungs.

Characterization of metastases in control animals

Based on the timeline study, a seeding period of 1, 2, and 3 weeks resulted in 37.5% (5 of 8), 100% (8 of 8), and 94% (15 of 16) of mice possessing metastases in their lungs (Fig. 2a). Overgrowth was seen for mice with 2 and 3 week seeding periods. At 2 weeks, 12.5% (1 of 8) of lungs were overgrown and at 3 weeks 18% (3 of 17) lungs were overgrown (data not shown). Whereas the mean number of metastases per lung was comparable at 2 (11.7) and 3 (10.9) weeks, the variance in metastases number was approximately three-fold greater at 3 weeks. The results are summarized in Fig. 2.

The effect of HIFU treatment on lung metastasis

No significant differences were found between total number of metastases counted under 100× magnification in control and treated groups. However, 46.7% (7/15) of the treated lungs and 13.3% (2/15) of the control lungs presented metastatic overgrowth (Fig. 3). The overall metastatic burden was evaluated by measuring total area of metastatic tissue compared to total area of lung tissue. Representative images and metastases masks for different levels of metastatic burden are shown in Fig. 4. No significant differences were observed between control and treated groups at any of the cutoffs, although there was ~30% greater metastases area fraction for the pulsed-HIFU treatment. Furthermore, there was a general trend of increased metastatic burden in the lungs of pulsed-HIFU treated mice in regards to mean number of metastases per lung and mean size of metastatic lesion. These results are summarized in Table 1 and Fig. 5.

Discussion

The goal of the study was to evaluate the effects of pulsed-HIFU exposures on the metastatic potential of solid tumors using a murine model. Based on previous studies of this nature [14–17], a standard experimental design was adopted with a well characterized metastatic primary tumor [19]. After reaching a required size or age, where consistent and predictable seeding of metastases occurred, the tumors were treated and the tumor bearing limb was resected 24 h later in order to allow metastases to develop following the exposures. At a set post-surgery date, the animals were then euthanized and the metastatic burden in the lungs was quantitatively assessed. Resection of the tumor bearing limb at a set time post-treatment provided a window of time for the treatment to influence metastatic potential. Delaying or not amputating the tumor bearing leg would allow the primary tumor to seed additional metastases and increase metastatic burden, confounding the results and potentially resulting in detrimental effect on the health of the mice. [15, 16].

Since this is the first report of the Mvt-1 cell line used in this manner, the initial objective of the study was to determine the time at which to treat and resect post-inoculation, as well as the necessary duration for development of lung metastases before euthanizing the animals and removing the lungs for analysis. This latter time point had to satisfy two criteria: (1) lung metastases must sufficiently develop to be analyzed and (2) the metastatic burden could not be too great since this overgrowth may confound the results. A multifactorial approach was taken where multiple combinations of treatment/resection periods (post-inoculation) and grow-out periods (post-surgery) were evaluated. The combination of the two periods chosen resulted in all animals with lung metastases and a minimal variance in the number of metastases compared to other combinations of time periods. The selection of these experimental parameters was further validated in a follow-up experiment, which examined treatment effects, where all control animals had quantifiable metastases, and lungs in only 2 of the 15 mice in the control group were overgrown.

The second objective of the study, and its main goal, was to determine if the pulsed-HIFU exposures were affecting the metastatic process. We attempted to determine the mean number of metastases in the lungs of the control and treated groups. Unfortunately, a large of number of treated mice had lungs where the metastatic burden presented itself not as individual and clearly defined lesions. Instead, large overgrown regions were observed, being the result of either more lesions that had grown into each other or the same number of lesions that had grown faster. As mentioned above, 2 of 15 mice in the control group had lungs that were overgrown; more than three times as many (7 of 15) were overgrown in the treated animals. Of the lesions that could be accurately counted, a greater number was found in the treated group compared to the controls; however, this difference was not significant. In light of the fact that so many of the lungs were overgrown, an overall assessment of metastatic burden may be better elucidated by calculating the metastatic area fraction of the lung. Digital images were captured of individual lung sections and these images were processed using custom designed image processing code. Presented as the mean area fraction of metastases, this value was ~30% greater in the treated mice. Although this difference in metastatic burden was not significant, such a marked increase may be clinically relevant. In fact, RECIST criteria defines progressive disease (PD) as the sum of the longest diameter (LD) of the target lesions increasing by 20% or more.

If indeed the pulsed-HIFU exposures did enhance the metastatic burden, where the level of variance did not allow for statistical significance, the question arises as to how pulsed-HIFU may influence metastatic burden. At least two theories can be conceived: One is that the exposures are causing the upregulation of genes or factors that may facilitate one or more stages of the metastatic process (e.g. proteases, which can facilitate adhesion, invasion, and survival of metastatic cells as well as angiogenesis and tumor progression, and hence increase metastatic burden [24–26]). HIFU exposures have shown the ability to cause significant upregulation of various genes, such as heat shock proteins (HSPs) [27], as well as other stress proteins (SPs) and glucose related proteins (GRPs) [28]. On the other hand, the exposures may be generating mechanical effects in the tissues, such as locally induced shear, which could also enable the detachment of cells from one another or the extracellular matrix, and ultimately facilitate infiltration and dissemination.

Acoustic cavitation is generally described as the formation, oscillation, and subsequent collapse of gas bubbles under the influence of the varying pressure field created by an ultrasound exposure. A variety of biological effects can be induced by both stable (non-inertial) and collapsing (inertial) bubbles, from temporarily permeabilizing cell membranes and the blood brain barrier to irreversible destruction of cells and large-scale necrosis and hemorrhage. Cavitation has been the most widely investigated non-thermal mechanism of ultrasound, and is generally thought to be the most important for inducing bio-effects [29]. As mentioned above, previous studies looking into the effects of pulsed focused ultrasound exposures did observe increases in metastasis. This occurred as a result of both pulsed-HIFU [15] and shock wave lithotripsy [17, 18]. In two of these studies [15, 18], experiments were designed to specifically look at the potential contributions of acoustic cavitation in this process, where ultrasound contrast agents were administered prior to the exposures. In both these studies, evidence was provided that clearly indicated that cavitation was, at least in part, playing a role.

Our lab has proposed a novel ultrasound mechanism for enhancing the permeability of the exposed tissues, leading to improved delivery and distribution of therapeutic agents [30]. This mechanism is based on the unidirectional, radiation forces generated in the tissues due to transfer of momentum during each HIFU pulse. These forces produce local displacements of tissue that may be on the order of tens to hundreds of microns [31]. The mechanism is based not on the extent of the displacements themselves, but instead on the large gradients in displacement that occur at the interface of the focal region and the tissue just outside of it. Here, local shear generated, and the resulting strain [32], is proposed to be working on the relatively weak structures in the tissue such as the junctions between cells and the extracellular matrix. We reported new evidence for the proposed mechanism by linking strain from locally induced shear to resulting structural effects (i.e. widened gaps between muscle fiber bundles in the calves of mice) [12]. These observations were further correlated with improved convective interstitial transport of fluorescently labeled nanospheres that were administered locally following the exposures. If such effects are also occurring in tumors between parenchymal cells, they could also be facilitating the dissemination of tumor cells and potentially exacerbating the metastatic process. Cezeaux et al. [33], for example, carried out studies using a parallel plate flow chamber looking at the effects of shear stress on cell detachment. They showed that the induced stress significantly increased detachment of cells when using highly metastatic ras-transformed cells compared to nonmetastatic normal cells.

Discussions so far have been in regards to how pulsed-HIFU exposures may be creating mechanical effects that can cause physical detachment of cells in order to exacerbate the metastatic process. Additional effects, however, may also be occurring through mechanotransduction, where external forces exerted on cells can create changes in cellular signaling, gene expression and function [34]. Integrins and cadherins, which are important attachment molecules that undergo changes in the metastatic process [35], have been associated with a variety of mechanotransduction phenomena, as well as fluid shear stress, elevated hydrostatic pressure and cellular responses to stretching [36]. In depth investigations on metastasis, looking at the effects of treatments that exert physical forces on solid tumors should ultimately explore the potential role of mechanotransduction responses.

Miller and Dou [15] found significantly higher numbers of metastases in their melanoma cell line B16-D5 tumor model following HIFU, whereas differences were not significant in the present study. These results may be perceived as perplexing seeing that their exposures were similar in regards to energy deposition and pressure amplitudes. If indeed mechanical effects were responsible, then not surprisingly the mechanical (e.g. elastic modulus) and biological (extracellular matrix) factors, which differ from tumor to tumor [37], could explain at least in part the difference in response.

In conclusion, the present study describes a process, model and method in which to quantify metastatic burden resulting from the effects of therapeutic interventions (in this case, pulsed-HIFU exposures). Furthermore, an image processing protocol was developed in order to reproducibly quantify and compare metastatic burden between groups, when simple counting of individual metastases was not possible. Regarding the effects of the particular pulsed-HIFU exposures that were used, a trend of increasing metastatic burden was observed in treated mice compared to controls; however, the differences were not significant. Moreover, increased numbers of mice in the treated group had overgrown metastatic burden in the lungs. Future studies are planned to evaluate the potential effects of varying the pulsed-HIFU exposures (duty cycle, frequency, or total acoustic power) to study potential influences on metastatic burden. Studies may also be carried out with other tumor models whose different mechanical and biological properties could provide further insight into potential mechanisms for pulsed-HIFU to influence metastases. Determining the proper conditions (exposures and tumor type) for pulsed-HIFU in the treatment of cancer will be essential in order for these exposures to be optimized to maximize delivery of therapeutics and minimize risk for worsening metastatic burden. The model developed in this study could also be used to assess other ablative therapies such as radiofrequency, microwave, or cryoablation, all in common clinical use, but with undefined influence on metastatic potential.

Acknowledgments

We would like to thank Dr Arnulfo Mendoza and Ms. Mary Angstadt for their technical assistance, and Dr Marius Linguraru for helpful consultations on image processing. This study was supported in part by Howard Hughes Medical Institute NIH Research Scholars Program (J.S.), and by the intramural research program of the NIH Clinical Center.

References

1. Kennedy J. High-intensity focused ultrasound in the treatment of solid tumours. Nat Rev Cancer. 2005; 5(4):321–327. doi: 10.1038/nrc1591. [PubMed: 15776004]
2. Frenkel V. Ultrasound mediated delivery of drugs and genes to solid tumors. Adv Drug Deliv Rev. 2008; 60(10):1193–1208. doi:10.1016/j.addr.2008.03.007. [PubMed: 18474406]
3. Wu F, Wang Z, Chen W, et al. Preliminary experience using high intensity focused ultrasound for the treatment of patients with advanced stage renal malignancy. The Journal of Urology. 2003; 170(6 Pt 1):2237–2240. doi:10.1097/01.ju.0000097123.34790.70. [PubMed: 14634387]
4. Kennedy J, Wu F, ter Haar G, et al. High-intensity focused ultrasound for the treatment of liver tumours. Ultrasonics. 2004; 42(1–9):931–935. [PubMed: 15047409]
5. Kratzik C, Schatzl G, Lackner J, et al. Transcutaneous high-intensity focused ultrasonography can cure testicular cancer in solitary testis. Urology. 2006; 67(6):1269–1273. doi:10.1016/j.urology.2005.12.001. [PubMed: 16678890]

6. Catane R, Beck A, Inbar Y, et al. MR-guided focused ultrasound surgery (MRgFUS) for the palliation of pain in patients with bone metastases–preliminary clinical experience. Ann Oncol. 2007; 18(1):163–167. doi:10.1093/annonc/mdl335. [PubMed: 17030549]
7. Miller D, Song J. Tumor growth reduction and DNA transfer by cavitation-enhanced high-intensity focused ultrasound in vivo. Ultrasound Med Biol. 2003; 29(6):887–893. doi:10.1016/S0301-5629(03)00031-0. [PubMed: 12837504]
8. Khaibullina A, Jang BS, Sun H, et al. Pulsed high-intensity focused ultrasound enhances uptake of radiolabeled monoclonal antibody to human epidermoid tumor in nude mice. J Nucl Med. 2008; 49(2):295–302. doi:10.2967/jnumed.107.046888. [PubMed: 18199622]
9. Poff J, Allen C, Traughber B, et al. Pulsed high-intensity focused ultrasound enhances apoptosis and growth inhibition of squamous cell carcinoma xenografts with proteasome inhibitor bortezomib. Radiology. 2008; 248(2):485–491. doi:10.1148/radiol.2482071674. [PubMed: 18574138]
10. Frenkel V, Li K. Potential role of pulsed-high intensity focused ultrasound in gene therapy. Future Oncol (Lond Engl). 2006; 2(1):111–119. doi:10.2217/14796694.2.1.111.
11. Chung B, Wiley JP. Extracorporeal shockwave therapy: a review. Sport Med (Auckl NZ). 2002; 32(13):851–865. doi:10.2165/00007256-200232130-00004.
12. Hancock HA, Smith LH, Cuesta J, et al. Investigations into pulsed-high intensity focused ultrasound enhanced delivery: preliminary evidence. Ultrasound Med Biol. 2009 in press.
13. Wu F, Wang ZB, Jin CB, et al. Circulating tumor cells in patients with solid malignancy treated by high-intensity focused ultrasound. Ultrasound Med Biol. 2004; 30(4):511–517. doi:10.1016/j.ultrasmedbio.2003.12.004. [PubMed: 15121253]
14. Oosterhof G, Cornel E, Smits G, et al. Influence of high-intensity focused ultrasound on the development of metastases. Eur Urol. 1997; 32(1):91–95. [PubMed: 9266238]
15. Miller D, Dou C. The potential for enhancement of mouse melanoma metastasis by diagnostic and high-amplitude ultrasound. Ultrasound Med Biol. 2006; 32(7):1097–1101. doi:10.1016/j.ultrasmedbio.2006.03.013. [PubMed: 16829323]
16. Miller D, Dou C. Contrast-aided diagnostic ultrasound does not enhance lung metastasis in a mouse melanoma tumor model. J Ultrasound Med. 2005; 24(3):349–354. [PubMed: 15723847]
17. Oosterhof GO, Cornel EB, Smits GA, et al. The influence of high-energy shock waves on the development of metastases. Ultrasound Med Biol. 1996; 22(3):339–344. doi:10.1016/0301-5629(95)02051-9. [PubMed: 8783466]
18. Miller DL, Dou C, Song J. Lithotripter shockwave-induced enhancement of mouse melanoma lung metastasis: dependence on cavitation nucleation. J Endourol. 2004; 18(9):925–929. doi:10.1089/end.2004.18.925. [PubMed: 15659934]
19. Pei X, Noble M, Davoli M, et al. Explant-cell culture of primary mammary tumors from MMTV-c-Myc transgenic mice. In Vitro Cell Dev Biol Anim. 2004; 40(1–2):14–21. [PubMed: 15180438]
20. Crawford NP, Qian X, Ziogas A, et al. Rrp1b, a new candidate susceptibility gene for breast cancer progression and metastasis. PLOS Genet. 2007; 3(11):e214. doi:10.1371/journal.pgen.0030214. [PubMed: 18081427]
21. Dromi S, Frenkel V, Luk A, et al. Pulsed-high intensity focused ultrasound and low temperature-sensitive liposomes for enhanced targeted drug delivery and antitumor effect. Clin Cancer Res. 2007; 13(9):2722–2727. doi:10.1158/1078-0432.CCR-06-2443. [PubMed: 17473205]
22. Dittmar K, Xie J, Hunter F, et al. Pulsed high-intensity focused ultrasound enhances systemic administration of naked DNA in squamous cell carcinoma model: initial experience. Radiology. 2005; 235(2):541–546. doi:10.1148/radiol.2352040254. [PubMed: 15798154]
23. Hong SH, Briggs J, Newman R, et al. Murine osteosarcoma primary tumour growth and metastatic progression is maintained after marked suppression of serum insulin-like growth factor I. Int J Cancer. 2009; 124(9):2042–2049. [PubMed: 19132750]
24. Purushothaman A, Chen L, Yang Y, et al. Heparanase stimulation of protease expression implicates it as a master regulator of the aggressive tumor phenotype in myeloma. J Biol Chem. 2008; 283(47):32628–32636. doi:10.1074/jbc.M806266200. [PubMed: 18812315]
25. Tripathi M, Nandana S, Yamashita H, et al. Laminin-332 is a substrate for hepsin, a protease associated with prostate cancer progression. J Biol Chem. 2008; 283(45):30576–30584. doi:10.1074/jbc.M802312200. [PubMed: 18784072]

26. Villares GJ, Zigler M, Wang H, et al. Targeting melanoma growth and metastasis with systemic delivery of liposome-incorporated protease-activated receptor-1 small interfering RNA. Cancer Res. 2008; 68(21):9078–9086. doi:10.1158/0008-5472.CAN-08-2397. [PubMed: 18974154]
27. Rome C, Couillaud F, Moonen CT. Spatial and temporal control of expression of therapeutic genes using heat shock protein promoters. Methods (S Diego Calif). 2005; 35(2):188–198. doi:10.1016/j.ymeth.2004.08.011.
28. Kramer G, Steiner GE, Grobl M, et al. Response to sub-lethal heat treatment of prostatic tumor cells and of prostatic tumor infiltrating T-cells. Prostate. 2004; 58(2):109–120. doi:10.1002/pros.10314. [PubMed: 14716736]
29. Kimmel E. Cavitation bioeffects. Crit Rev Biomed Eng. 2006; 34(2):105–161. [PubMed: 16749890]
30. Frenkel V, Oberoi J, Stone MJ, et al. Pulsed high-intensity focused ultrasound enhances thrombolysis in an in vitro model. Radiology. 2006; 239(1):86–93. doi:10.1148/radiol.2391042181. [PubMed: 16493016]
31. Lizzi FL, Muratore R, Deng CX, et al. Radiation-force technique to monitor lesions during ultrasonic therapy. Ultrasound Med Biol. 2003; 29(11):1593–1605. doi:10.1016/S0301-5629(03)01052-4. [PubMed: 14654155]
32. Palmeri ML, McAleavey SA, Fong KL, et al. Dynamic mechanical response of elastic spherical inclusions to impulsive acoustic radiation force excitation. EEE Trans Ultrason Ferroelectr Freq Control. 2006; 53(11):2065–2079. doi:10.1109/TUFFC.2006.146.
33. Cezeaux JL, Austin V, Hosseinipour MC, et al. The effects of shear stress and metastatic phenotype on the detachment of transformed cells. Biorheology. 1991; 28(3–4):195–205. [PubMed: 1932712]
34. Chen CS. Mechanotransduction—a field pulling together? J Cell Sci. 2008; 121(Pt 20):3285–3292. doi:10.1242/jcs.023507. [PubMed: 18843115]
35. Steeg P. Tumor metastasis: mechanistic insights and clinical challenges. Nat Med. 2006; 12(8):895–904. doi:10.1038/nm1469. [PubMed: 16892035]
36. Schwartz MA, DeSimone DW. Cell adhesion receptors in mechanotransduction. Curr Opin Cell Biol. 2008; 20(5):551–556. doi:10.1016/j.ceb.2008.05.005. [PubMed: 18583124]
37. Netti PA, Berk DA, Swartz MA, et al. Role of extracellular matrix assembly in interstitial transport in solid tumors. Cancer Res. 2000; 60(9):2497–2503. [PubMed: 10811131]

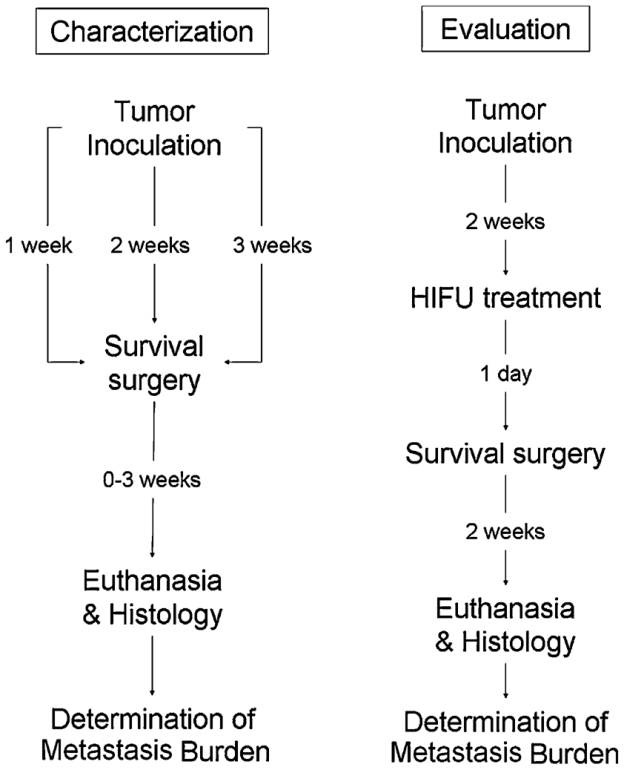

Fig 1.

Experimental design. A preliminary study (*left*) was used to characterize the tumor model and determine the optimal duration of primary tumor growth for consistent seeding of metastases (ending at surgeries), and sufficient grow out period (ending at euthanasia) for quantitative analysis of lung metastases. Based on this characterization, a study to evaluate the effects of pulsed-HIFU exposures was designed (*right*) where a 2 weeks primary tumor growth period and a 2 weeks metastatic growth period was employed

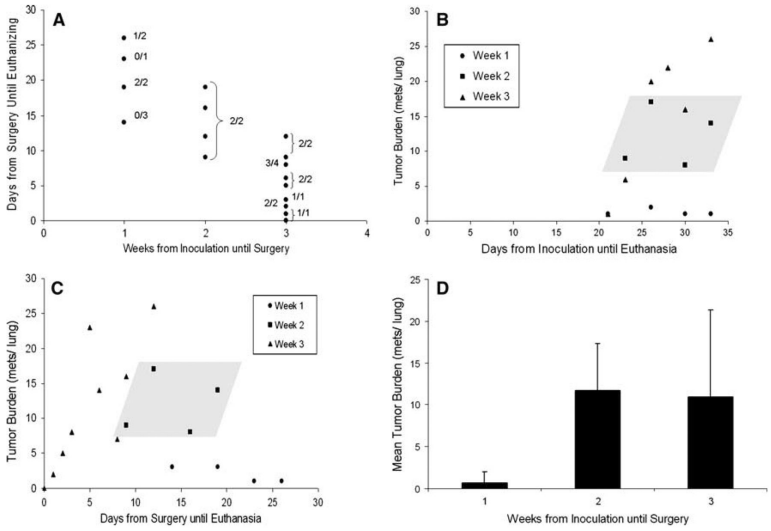

Fig. 2.

Characterization of lung metastases in control animals. **a** Experimental design showing the combination of grow out periods for primary tumors (weeks from inoculation until survival surgery) and metastases (days from surgeries until euthanasia). The numerator of the fractions indicates the number of mice in which metastases were found in proportion to the total number (denominator) evaluated. **b** Tumor burden as a function of days from primary tumor inoculation until mice were euthanized. Data is presented according to the week when surgeries were performed. **c** Tumor burden as a function of days from surgery until mice were euthanized. Data is presented according to the week when surgeries were performed. For **b** and **c**, the *shaded parallelogram* includes all data points for week 2. **d** Mean tumor burden as a function of the week that surgeries were performed

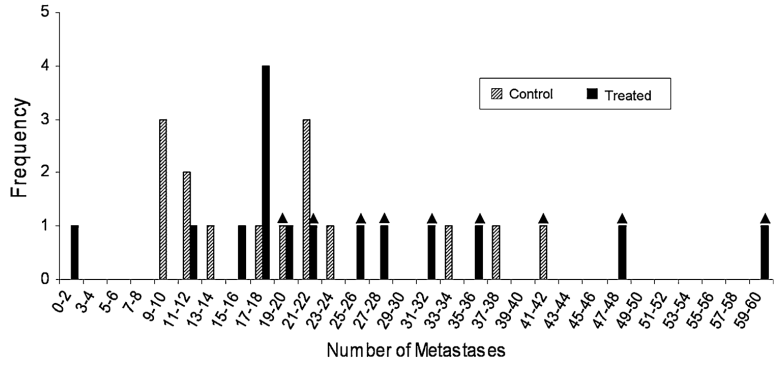

Fig. 3.

Distribution of mean number of metastases per lung in control (n = 15) and treated (n = 15) groups. The *triangle* over individual *bars* indicates lungs that possessed overgrown regions, therefore making it more difficult to accurately count the number of individual metastases. Only clearly defined metastatic lesions were counted. Of the treated lungs 7 out of 15 were overgrown, whereas only 2 out of 15 control lungs were overgrown. This difference was, however, not statistically significant

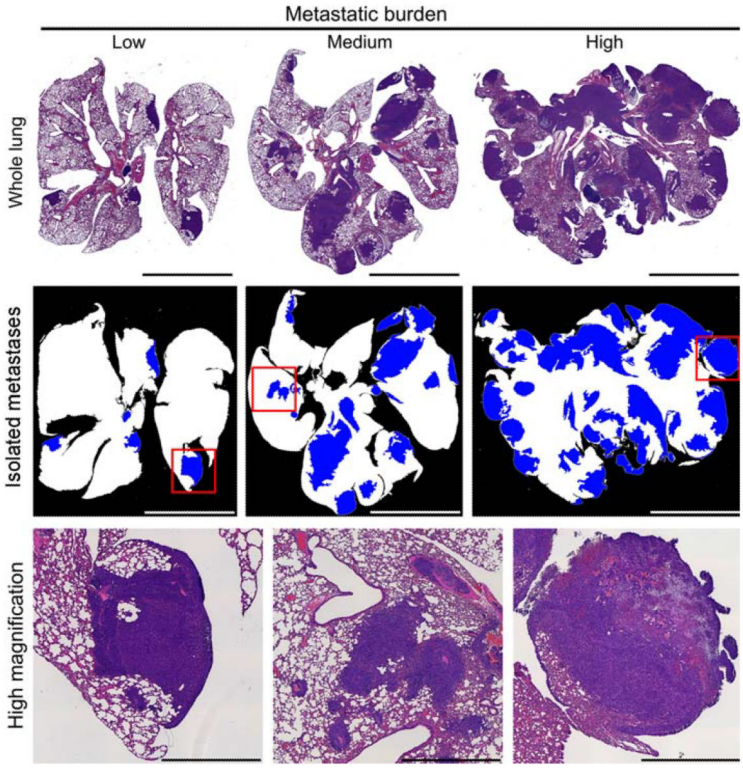

Fig. 4.

Histology and image processing. (*upper*) Representative images of whole lungs, showing low, medium and high metastatic burden. (*middle*) Masks produced with image processing showing healthy lung (*white*) and metastases (*blue*) at a cutoff limit of 0.1 mm^2. (*lower*) High magnification of *boxes* from respective *middle* images. *Left* image shows a clearly defined metastatic lesion; *middle* image shows a not clearly defined lesion that could be multiple lesions grown into each other; *right* image shows a large lesion that has become necrotic (*upper right* region). *Bar* = 5 mm (*upper* and *middle*); 1 mm (*lower*)

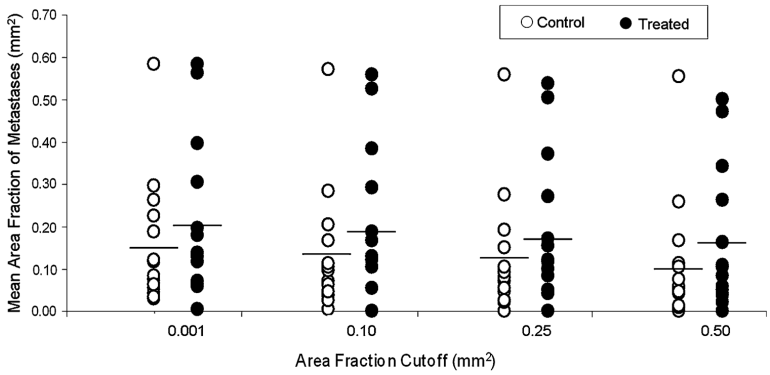

Fig. 5.

Mean area fraction of metastases for each lung in control (n = 15) and treated (n = 15) groups. `Cutoff' limits for image processing of individual lesion surface areas were 0.001, 0.10, 0.25 and 0.5 mm^2. No significant differences were found between control and treated groups at each of the cutoffs. *Horizontal bars* indicate means

Table 1

The effect of HIFU treatment on lung metastasis

0.001		0.1		0.25		0.5	
Control	**Treated**	**Control**	**Treated**	**Control**	**Treated**	**Control**	**Treated**
Mean area fraction of metastases							
0.15	0.20	0.13	0.17	0.12	0.16	0.11	0.14
Mean number of metastases per lung							
133.7	108.8	11.7	13.2	7.4	8.8	5.0	6.1
Mean size of metastatic lesion (mm^2)							
0.08	0.11	0.74	0.86	1.09	1.20	1.44	1.58

Data is provided for four individual cutoff limits (in mm^2) used in the image processing procedure (n = 15)